INVESTIGATING VEHICLE MODEL DETAIL FOR CLOSE TO LIMIT MANEUVERS AIMING AT OPTIMAL CONTROL

Kristoffer Lundahl, Jan Åslund, Lars Nielsen
Department of Electrical Engineering, Linköping University
581 83 Linköping, Sweden
kristoffer.lundahl@liu.se

Abstract

In advanced road vehicle safety systems it is imperative to have a model describing the vehicle motions and behaviors with sufficient precision. Often a model incorporating a higher level of complexity generates more accurate data, with the disadvantage of demanding additional calculation power. This study will therefore focus on investigating how models of different detail level represents the vehicle behavior, for maneuvers going from moderate to more aggressive. The characteristics in particular investigated are tire saturation, tire force lag and the effect of load transfers. A vehicle testbed has also been developed, making model validations towards experimental data available.

1 INTRODUCTION

With recent advances in sensor technology, future vehicles will have, for instance, 6D IMU:s and GPS as standard sensors. This will open up for improved control at critical maneuvers, but the classical vehicular dynamic models given in text books are not necessarily the most suitable for these future applications, e.g. since the models should be tractable to calculation of optimal maneuvers and to generation of the right driving feel both in driving simulators and in vehicle handling. There will be a need for new classes of models tailored to the problems of study. The models rely on nominal parameters, and some of these are uncertain (tire radii, inertia, body mass, air drag), while other naturally varies over time (load, tire-road friction, tire stiffness), but on different time scales. Appropriate models can open up new approaches to adaptively estimate these. LiU has started a program investigating expressiveness of models compared to real data from an advanced test vehicle, and here the experimental facilities and first results are reported.

The results will be useful for several projects ranging from sensor informatics, over quantified driving feel, to various optimal control problems.

2 EXPERIMENTS

Data presented in this study is gathered with the LiU Research Vehicle, a testbed developed for vehicle dynamics studies, see Figure 1. This vehicle is essentially a Volkswagen Golf IV (2008) equipped with a set of external sensors, where the main setup consists of an optical slip angle sensor (Corrsys-Datron S-350), optical pitch/roll angle sensors (3 Corrsys-Datron HF500C), IMU (Xsens MTi) and GPS (u-blox AEK-4P). In addition, access to the vehicle CAN bus gives the possibility to sample data from the vehicle internal sensors, steering wheel angle being the most relevant for this work.

Figure 1: The LiU Research Vehicle, a vehicle testbed developed for vehicle dynamics studies.

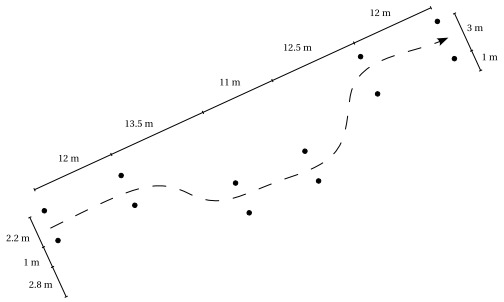

Figure 2: Double lane change test track.

2.1 Experiment procedure

For this study in particular two tests were analyzed, a constant radius test and a double lane change test. The tests were performed on high quality asphalt surface at a vehicle race/test facility.

Constant radius

This test is used for evaluating the steady state under-/oversteer behavior of the vehicle at different lateral acceleration. The measurement sampling of this test was done at a roundabout-like part of the track, for different speeds.

Double lane change

The double lane change test carried out for this study is based on the standardized ISO 3888-2 test [1], developed for vehicle stability evaluation. This test is particularly good for evaluating fast transient behavior, while the vehicle also experiences both under- and oversteering behavior throughout the test.

In contrast to the original test, the test track setup was here mirrored, see Figure 2, and also the clutch was disengaged when initiating the test, to minimize the longitudinal effects.

3 VEHICLE MODELS

In this study, four different models with varying detail level are evaluated. Three of which are based on the single track model, using different tire models, while the fourth is a double track model, capturing the lateral load transfers.

3.1 Single track model

The basic motion equations for the single track model is described by equation 1 and 2 [2]. The lateral forces, $F_{y,f}$ and $F_{y,r}$, are given by the different tire models below, together with the slip angles defined in equation 3.

$$m\dot{v_y} + mv_x\dot{\psi} = F_{y,f} + F_{y,r} \tag{1}$$

$$I_z\ddot{\psi} = F_{y,f}l_f - F_{y,r}l_r \tag{2}$$

$$\alpha_f = \delta - \frac{v_y + l_f\dot{\psi}}{v_x}, \quad \alpha_r = -\frac{v_y - l_r\dot{\psi}}{v_x} \tag{3}$$

Linear tire model

The linear tire model has a linear relation between lateral force and slip angle, equation 4, which together with the motion equations above gives a linear system that can be handled with quite low computational effort [2].

$$F_{y,i} = C_{\alpha,i}\alpha_i, \quad i = f, r \tag{4}$$

Magic Formula tire model

To capture the tire nonlinearities, essentially the force saturation, a nonlinear tire model is used, the Magic Formula tire model [3]. The model is implemented as equation 5 – 7.

$$F_{z,f} = \frac{l_r}{l_f + l_r}mg, \quad F_{z,r} = \frac{l_f}{l_f + l_r}mg \tag{5}$$

$$B_i = \frac{C_{\alpha_i}}{C\mu F_{z,i}} \tag{6}$$

$$F_{y,i} = \mu F_{z,i}\sin(C\arctan(B_i\alpha_i)), \quad i = f, r \tag{7}$$

Tire force lag

An interesting dynamic effect is the tire force lag, i.e. the time it takes for the tire to develop the force corresponding to the applied slip angle. As proposed in [4], this is modeled as a relaxation length, σ, delaying the effective slip angle, α', see equation 8 and 9.

$$\dot{\alpha_i'} = -\frac{v_x}{\sigma}(\alpha_i' + \alpha_i) \tag{8}$$

$$F_{y,i} = \mu F_{z,i}\sin(C\arctan(B_i\alpha_i')), \quad i = f, r \tag{9}$$

3.2 Double track model

To allow for a normal load dependent tire model, the vehicle model needs to be able to describe the load transfers between the wheels. Since this study focuses on lateral behavior, only the lateral load transfer is considered. The double track model used here achieves this by including the roll dynamics in the vehicle motion equations, equation 15 – 17. After the independent normal loads are known, the tire forces can be calculated as functions of normal load and slip angle, equation 14, as proposed in [4].

To the front slip angle equation, equation 10, a compliance term has been added, which, as stated in [5], can have a very important role in describing vehicle behavior. In the previous models, where separate tire properties are used for front and rear, this compliance can be captured by the front cornering stiffness, while in the double track model all four wheels use the same tire properties, making it necessary to introduce this term.

$$\alpha_1 = \alpha_2 = \delta - \frac{v_y + l_f\dot{\psi}}{v_x} - c_\delta(F_{y,1} + F_{y,2}), \quad \alpha_3 = \alpha_4 = -\frac{v_y - l_r\dot{\psi}}{v_x} \tag{10}$$

$$\Delta F_{z,i} = \frac{1}{t_i}(k_{\varphi,i}\varphi + ma_y h_{rc}), \quad i = f, r \tag{11}$$

$$F_{z,1/2} = F_{z,f} \pm \Delta F_{z,f}, \quad F_{z,3/4} = F_{z,r} \pm \Delta F_{z,r} \tag{12}$$

$$C_{\alpha,i} = c_1 c_2 F_{z,0} \sin\left(2\arctan\left(\frac{F_{z,i}}{c_2 F_{z,0}}\right)\right), \quad B_i = \frac{C_{\alpha_i}}{C\mu F_{z,i}} \tag{13}$$

$$F_{y,i} = \mu F_{z,i} \sin(C\arctan(B_i\alpha_i)), \quad i = 1, 2, 3, 4 \tag{14}$$

$$m\dot{v_y} + mv_x\dot{\psi} - mh\ddot{\varphi} = F_{y,1} + F_{y,2} + F_{y,3} + F_{y,4} \tag{15}$$

$$I_z\ddot{\psi} = (F_{y,1} + F_{y,2})l_f - (F_{y,3} + F_{y,4})l_r \tag{16}$$

$$I_x\ddot{\varphi} + (c_{\varphi,f} + c_{\varphi,r})\dot{\varphi} + (k_{\varphi,f} + k_{\varphi,f})\varphi = mgh\varphi + mh\dot{v_y} + mhv_x\dot{\varphi} \tag{17}$$

3.3 Model parameters

The vehicle parameters, presented in Table 1, has been given by manufacturer specifications, been measured or estimated from measurements. The tire parameters in Table 2 have all been estimated with various methods from measurement data. For example, Figure 3 shows measurements from several double lane change maneuvers, representing the front and rear axle slip angle versus lateral force relation. The data is normalized, as proposed in [4, 6], thus only representing the shape factor, C, in the Magic Formula model. In addition to the measurements, the normalized Magic Formula model using the shape factor seen in Table 2, is visualized.

Table 1: Vehicle parameters

Variable	*Value*	*Description*
m	1425 kg	Total vehicle mass
l_f	1.03 m	CG to front axle
l_r	1.55 m	CG to rear axle
t_f	1.54 m	Front track
t_r	1.52 m	Rear track
I_z	2500 kgm^2	Inertia about z-axis
I_x	550 kgm^2	Inertia about x-axis
$k_{\varphi,f}$	46.1 kNm/rad	Front roll stiffness
$k_{\varphi,r}$	30.7 kNm/rad	Rear roll stiffness
$c_{\varphi,f}$	1800 kNms/rad	Front roll damping
$c_{\varphi,r}$	1200 kNms/rad	Rear roll damping
h	0.4 m	Roll center to CG
h_{rc}	0.1 m	Roll center height

Table 2: Tire parameters

Variable	*Value*	*Description*
$C_{\alpha,f}$	108.5 kN/rad	Front cornering stiffness
$C_{\alpha,r}$	118.6 kN/rad	Rear cornering stiffness
μ	0.95	Friction coefficient
C	1.455	Magic Formula shape factor
σ	0.4 m	Relaxation length
c_1	13.5	Cornering stiffness factor
c_2	1.33	Cornering stiffness factor
F_{z0}	4000 N	Nominal normal load
c_δ	$2.5{\cdot}10^{-6}$ rad/N	Steer compliance

4 MODEL EVALUATION

In this section the models presented above are evaluated towards measurement data gathered from the earlier described experiments. The constant radius test is used for steady state evaluations, while the double lane change test is used when evaluating the transient response.

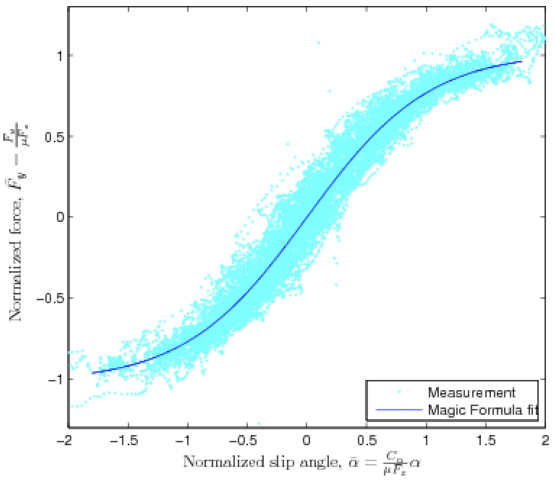

Figure 3: Magic Formula fit to normalized force, $\bar{F}_y$, and slip angle, $\bar{\alpha}$, measurements for front and rear suspension.

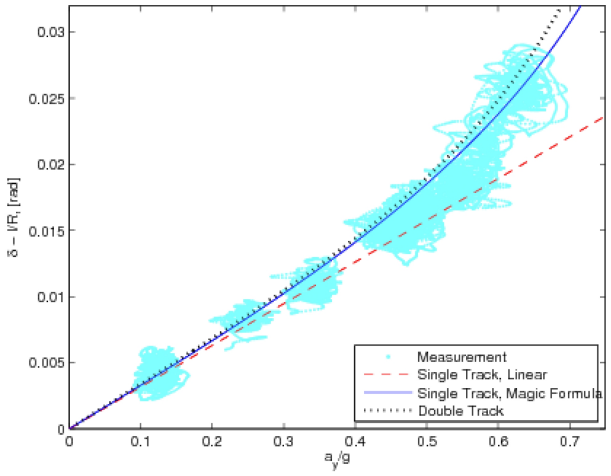

Figure 4: Handling diagram comparing the models' understeer behavior with measurements.

4.1 Steady state response

The handling diagram in Figure 4 shows the balance of the vehicle throughout the range of lateral accelerations. The vertical axis displays the difference between steering wheel angle, δ, and the quotient of wheel base, l, and cornering radius, R. This quantity is also equal to the difference between front and rear slip angles, $\alpha_f - \alpha_r$, and describes the under-/oversteer behavior. In this figure experiments from several constant radius tests are displayed, together with the calculated steady state characteristics of the models (the tire force lag model is excluded, since it has no effect in steady state conditions). This diagram shows that all models describes the vehicle balance very similar, and quite accurate, for small accelerations. However, at around $0.5g$'s the linear model starts to deviate a considerable amount from the behavior demonstrated by the experimental data, while the nonlinear models continues to have a fairly good fit.

What can also be seen is the double track demonstrating a slightly more understeered behavior than the nonlinear single track model, which can be derived from the tire force reduction, due to lateral load transfer, is larger at the front axle.

4.2 Transient response

The transient behavior of the simulation models is here evaluated towards experimental data for three double lane change tests, with alternating initial velocities, thus achieving various levels of maneuver aggression. Figure 5 – 7 presents the measurement data together with simulation results for these tests. All simulations have been fed with steering wheel input and longitudinal velocity from the measurements.

The quantities shown in Figure 5 – 7 are steer angle, yaw rate as well as front and rear slip angles. The steer angle is sampled from the vehicle internal sensors, measuring the steering wheel angle, and calculated to represent a lumped steer angle for the front wheels. The yaw rate is measured with an external IMU, mounted near the vehicle's center of gravity. The slip angles are measured with the optical slip angle sensor at the front of the car, then translated with yaw rate to represent the front and rear axle slip angles.

Test 1

Starting by studying the least aggressive of the tests, *Test 1*, Figure 5 shows results from all four models compared with measurements. This test has a peak lateral acceleration of $0.63g$, which is above the roughly stated limit (of $\sim 0.5g$) in section 4.1 for when the linear model still is a decent approximation (in the steady state condition). This can also be seen around time instances $t = 2.3$ and $t = 3.9$, where the linear model has a higher cornering stiffness resulting in smaller slip angles (most clearly visible for the front slip angle). However, since the vehicle operates in this region for a very short while, the omitting of force saturation in the linear model does not affect the behavior of the model very much.

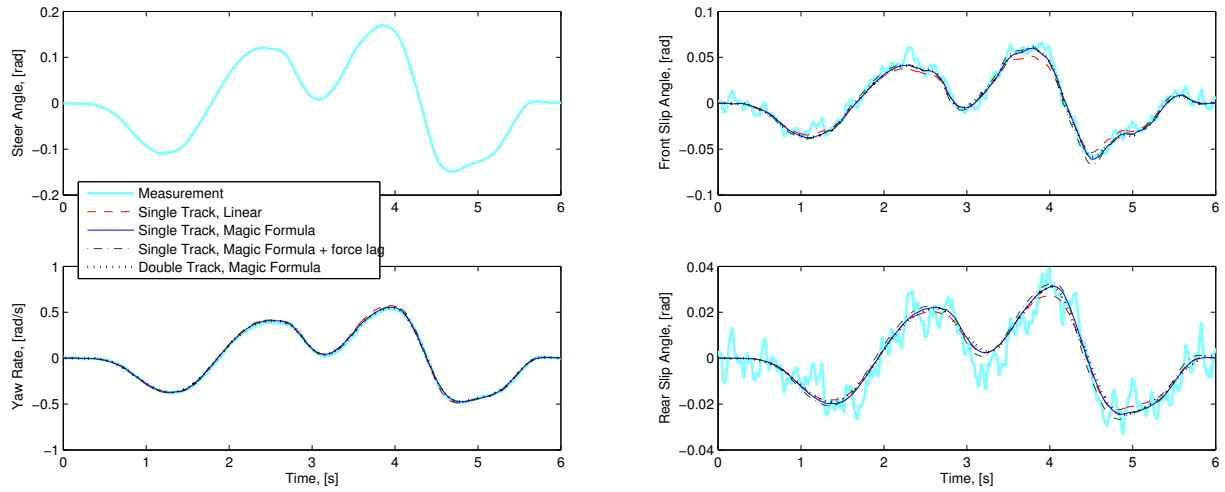

Figure 5: Test 1: $v_{init} = 36$ km/h, $a_{y,peak} = 6.2$ m/s^2. Double lane change test, experimental data and simulation results for all models.

Test 2

Moving on to *Test 2*, Figure 6, the vehicle now operates outside the "linear region", for longer intervals as well as further away from it. Thus, the linear single track model gives very erroneous results, where the smaller slip angles (compared to measurement) indicates the cornering stiffnesses being too stiff. The nonlinear models, giving similar output, manage to captures most of the stiffness saturation and represents both slip angles fairly good, except for the dip in both front and rear at $t = 3.5$.

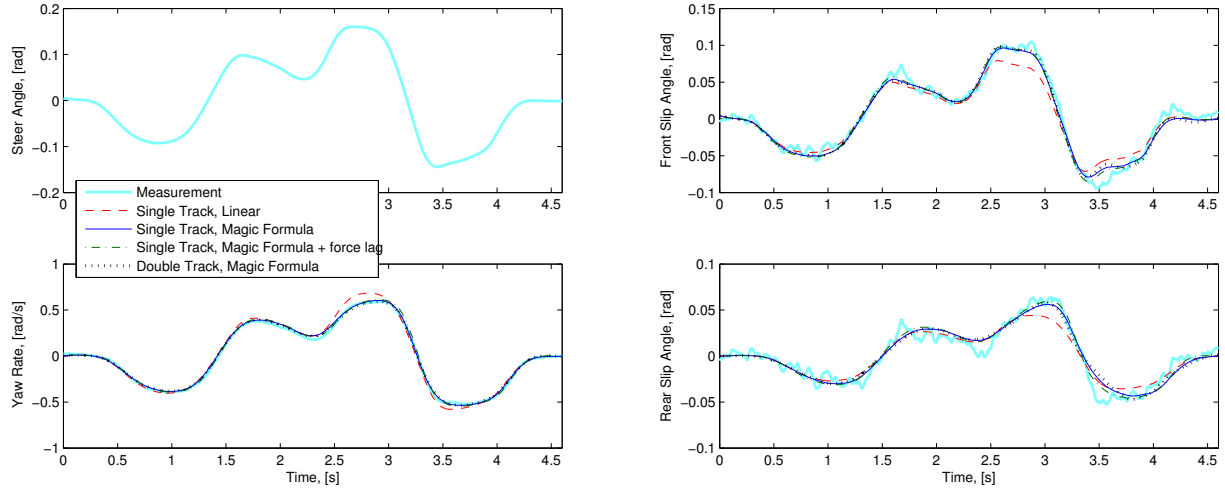

Figure 6: Test 2: $v_{init} = 49$ km/h, $a_{y,peak} = 8.5$ m/s^2. Double lane change test, experimental data and simulation results for all models.

Test 3

For *Test 3*, Figure 7, the linear model now deviates very much from the measurements, while the nonlinear models manage to capture the essential behavior of the measurements.

Looking at the front slip angle, all three nonlinear models are outputting very similar results, corresponding quite well to the measurements. For the rear slip angle, the single track model without force lag and the double track model again demonstrates more or less the same behavior. The force lag model, however, display a different rear slip angle behavior. It develops slightly higher peaks, especially at the peak around $t = 3.5$, imitating the measurement better than

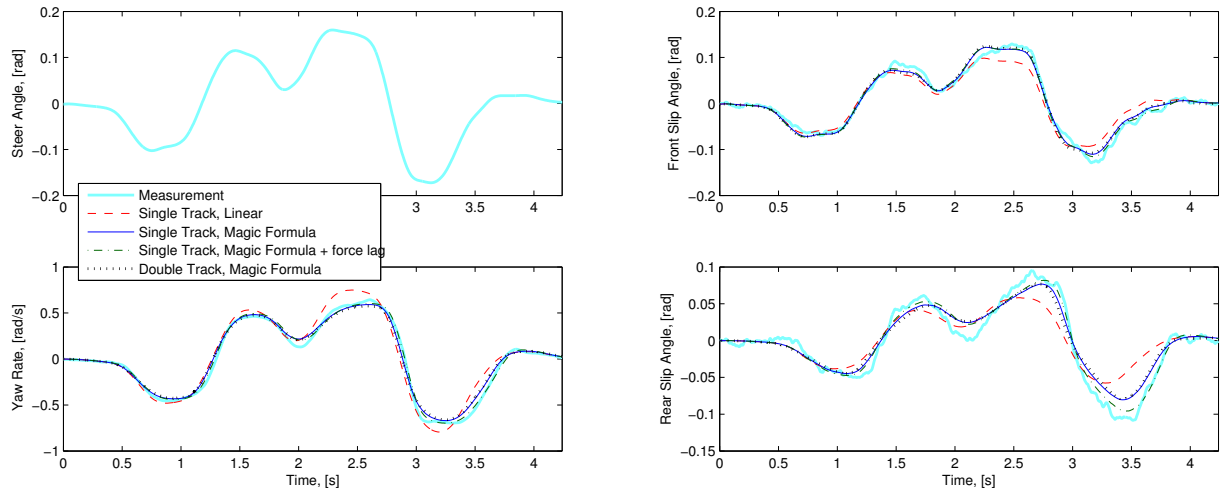

Figure 7: Test 3: $v_{init} = 59$ *km/h,* $a_{y,peak} = 9.9$ *m/s*^{2}*. Double lane change test, experimental data and simulation results for all models.*

the other models. This model also experience quicker transients, closer to what the measurement data demonstrates. These behaviors translate to a more accurate yaw rate for the force lag model, which especially can be seen between $t = 2.7$ and $t = 3.8$.

What none of the models manage to capture is the dip in rear slip angle midway through the test, at $t = 2$. This can also to some extent be seen for the previous two tests, and seems to be a consequence of the models experiencing a too stiff rear cornering stiffness at this very moment. Also, during the transients, especially for *Test 3*, the measurement show a much faster rear slip angle response than any of the models.

5 CONCLUSIONS

For vehicle maneuvers similar to *Test 2*, the most important property, captured by the nonlinear models, is the force saturation, while extending the model complexity, in the manner this study suggests, will not increase the model accuracy. When instead considering maneuvers of the same nature as *Test 3*, the force lag model appears to be the most accurate one. At the same time, the far more complex double track model is not able to enhance the accuracy compared to the single track with Magic Formula model. This should be considered when trying to gain accuracy by extending a model of simple structure, since the most natural step to take, which also quite often is suggested by literature, is to model all four wheels.

6 ACKNOWLEDGMENT

The authors would like to pay their gratitude to NIRA Dynamics, for technical support, and Linköpings Motorsällskap, for the providing of their test track facilities.

REFERENCES

[1] "ISO 3888-2:2011: Passenger cars – test track for a severe lane-change manoeuvre – part 2: Obstacle avoidance."

[2] J. R. Ellis, *Vehicle Handling Dynamics*. Mechanical Engineering Publications Limited, 1994.

[3] E. Bakker, L. Nyborg, and H. B. Pacejka, "Tyre modelling for use in vehicle dynamics studies," *SAE*, no. 870421, 1987.

[4] H. B. Pacejka, *Tire and vehicle dynamics*. SAE, 2002.

[5] M. C. Best, "Identifying tyre models directly from vehicle test data using an extended kalman filter," *Vehicle System Dynamics*, vol. 48, no. 2, 2010.

[6] W. F. Milliken and D. L. Milliken, *Race Car Vehicle Dynamics*. SAE International, 1995.